Electronic properties of graphene - I

Vladimir Falko

helped by
V.Cheianov, E.McCann
K.Kechedzhi, D.Abergel
T.Ando, B.Altshuler, I.Aleiner

Ultra-thin graphitic films: from flakes to micro-devices

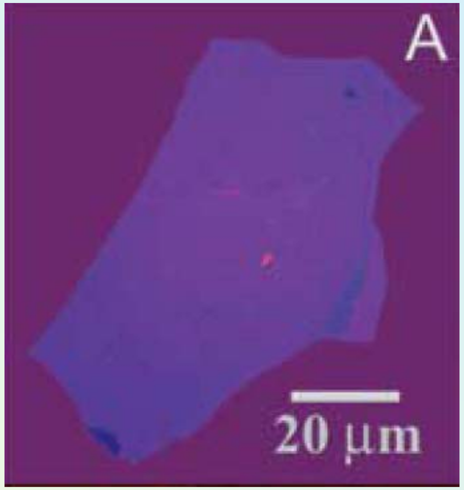

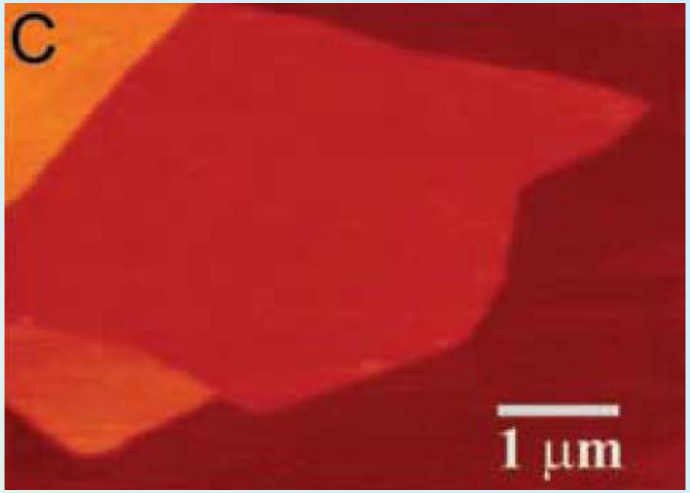

Novoselov *et al* -
Science 306, 666 (2004)

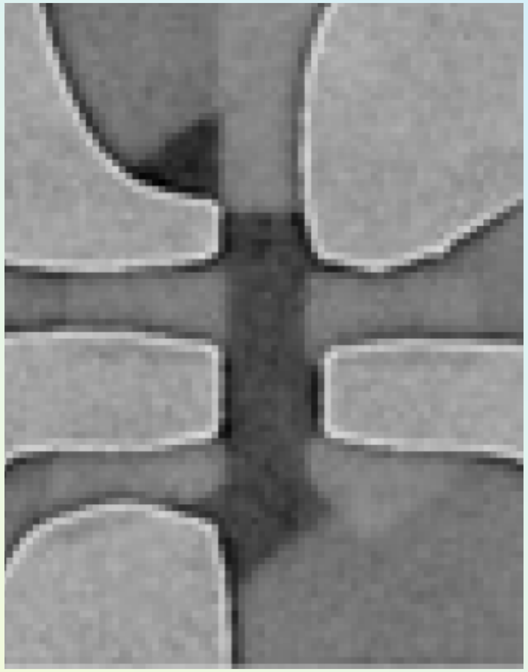

for references, see the review article
Geim and Novoselov - Nature Mat. 6, 183 (2007)

L1: band structure of monolayer graphene, 'chiral' electrons, Berry's phase π in monolayer graphene, unusual properties of the PN junction in graphene.

L2: bilayer graphene and QHE in graphene.

L3: disorder and transport in graphene.

Monolayer graphene

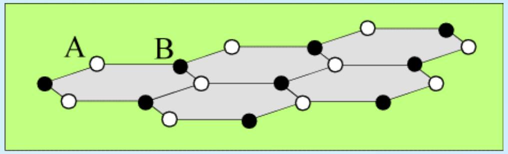

Lattice, symmetry and band structure of monolayer graphene.

Intricate details: trigonal warping in the band structure.

'Chiral' electrons and Berry's phase π in monolayer graphene, suppressed backscattering of chiral electrons.

Unusual properties of the PN junction in graphene focusing & caustics, Veselago lens for electrons.

Carbon has 4 electrons in the outer s-p shell

sp^2 **hybridisation forms strong directed bonds which determine a honeycomb lattice structure.**

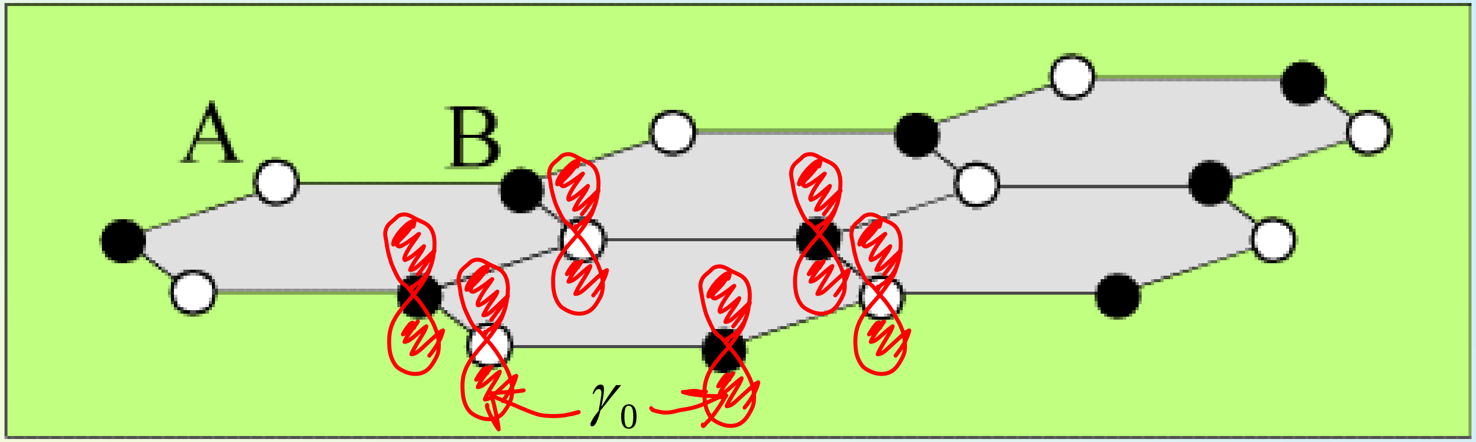

$p^z(\pi)$ **orbitals determine conduction properties of graphite**

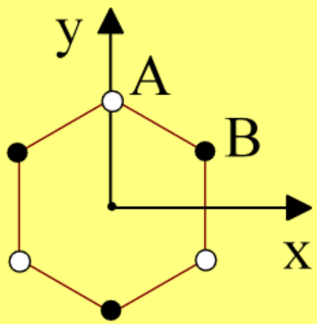

Two non-equivalent carbon positions

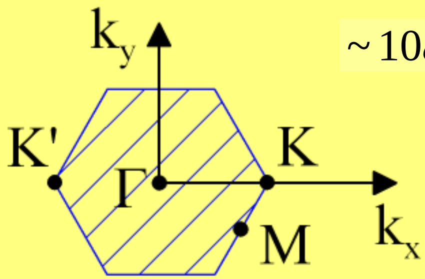

Two non-equivalent K-points

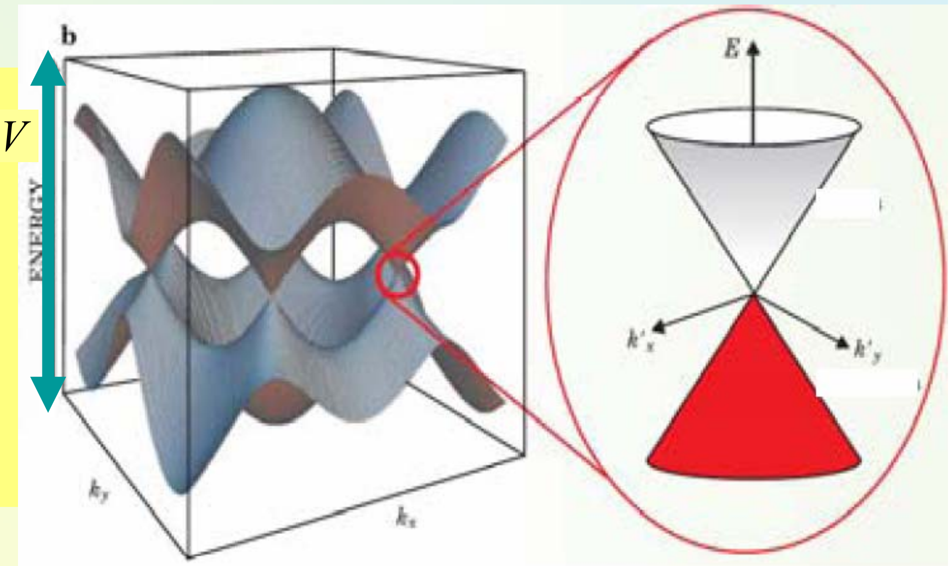

Wallace, Phys. Rev. 71, 622 (1947)
Slonczewski, Weiss, Phys. Rev. 109, 272 (1958)

Transfer integral on a hexagonal lattice

$$\mathcal{H}_{AB} = \langle \Phi_A | H | \Phi_B \rangle$$

$$\mathcal{H}_{AB} = \frac{1}{N} \sum_{\mathbf{R}_A}^{N} \sum_{\mathbf{R}_B}^{N} e^{i\mathbf{k}.(\mathbf{R}_B - \mathbf{R}_A)} \underbrace{\langle \phi_A(\mathbf{r}-\mathbf{R}_A) | H | \phi_B(\mathbf{r}-\mathbf{R}_B) \rangle}_{\gamma_0}$$

sum over 3 nearest neighbour positions

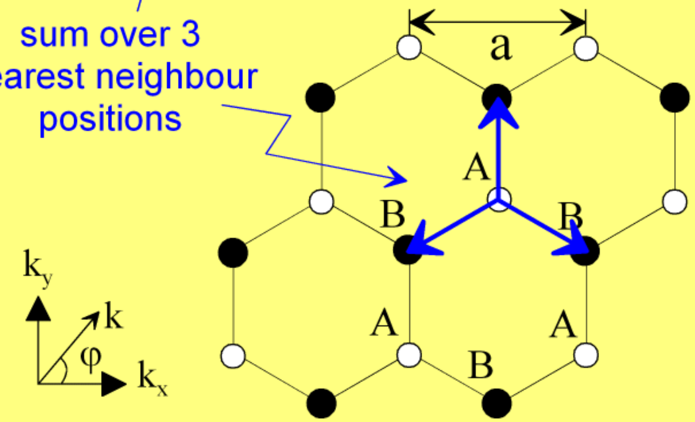

$$\mathcal{H}_{AB} = -\gamma_0 f(\mathbf{k}) \; ; \quad \mathcal{H}_{BA} = -\gamma_0 f^*(\mathbf{k})$$

$$f(\mathbf{k}) = e^{ik_y a/\sqrt{3}} + 2e^{-ik_y a/2\sqrt{3}} \cos(k_x a/2)$$

Tight binding model of a monolayer

Saito *et al*, "Physical Properties of Carbon Nanotubes" (Imperial College Press, London, 1998): Chapter 2.

Bloch function
$$\Phi_j(\mathbf{k}, \mathbf{r}) = \frac{1}{\sqrt{N}} \sum_{\mathbf{R}_j}^{N} e^{i\mathbf{k}.\mathbf{R}_j} \phi_j(\mathbf{r}-\mathbf{R}_j)$$

sum over N atomic positions

j^{th} atomic orbital: j = A or B

Eigenfunction
$$\Psi_j(\mathbf{k}, \mathbf{r}) = \sum_{i=1}^{2} C_{ji}(\mathbf{k}) \Phi_i(\mathbf{k}, \mathbf{r})$$

Transfer integral matrix $\quad \mathcal{H}_{ij} = \langle \Phi_i | H | \Phi_j \rangle$

Overlap integral matrix $\quad S_{ij} = \langle \Phi_i | \Phi_j \rangle$

Column vector $\quad C_j = \begin{pmatrix} C_{j1} \\ C_{j2} \end{pmatrix}$

Eigenvalue equation
$$\mathcal{H} C_j = \varepsilon_j S C_j$$

Wallace, Phys. Rev. 71, 622 (1947)
Slonczewski, Weiss, Phys. Rev. 109, 272 (1958)

Transfer integral on a hexagonal lattice

$$\mathcal{H}_{AB} = \langle \Phi_A | H | \Phi_B \rangle$$

$$\mathcal{H}_{AB} = \frac{1}{N} \sum_{\mathbf{R}_A}^{N} \sum_{\mathbf{R}_B}^{N} e^{i\mathbf{k}.(\mathbf{R}_B - \mathbf{R}_A)} \underbrace{\langle \phi_A(\mathbf{r}-\mathbf{R}_A) | H | \phi_B(\mathbf{r}-\mathbf{R}_B) \rangle}_{\gamma_0}$$

sum over 3 nearest neighbour positions

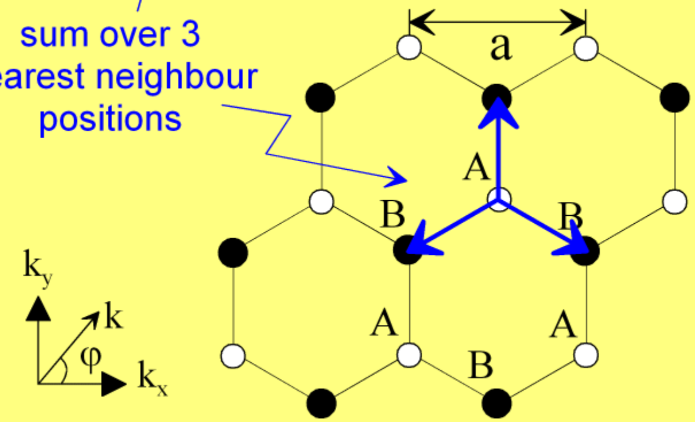

$$\mathcal{H}_{AB} = -\gamma_0 f(\mathbf{k}) \; ; \quad \mathcal{H}_{BA} = -\gamma_0 f^*(\mathbf{k})$$

$$f(\mathbf{k}) = e^{ik_y a/\sqrt{3}} + 2e^{-ik_y a/2\sqrt{3}} \cos(k_x a/2)$$

Tight binding model of a monolayer

Saito *et al*, "Physical Properties of Carbon Nanotubes" (Imperial College Press, London, 1998): Chapter 2.

Transfer integral matrix $\quad \mathcal{H} = \begin{pmatrix} 0 & -\gamma_0 f(\mathbf{k}) \\ -\gamma_0 f^*(\mathbf{k}) & 0 \end{pmatrix}$

Overlap integral matrix $\quad \mathcal{S} = \begin{pmatrix} 1 & s f(\mathbf{k}) \\ s f^*(\mathbf{k}) & 1 \end{pmatrix}$

Eigenvalue equation $\quad \mathcal{H} C_j = \varepsilon_j \mathcal{S} C_j$

$$\varepsilon = \frac{\pm \gamma_0 |f(\mathbf{k})|}{1 \mp s |f(\mathbf{k})|}$$

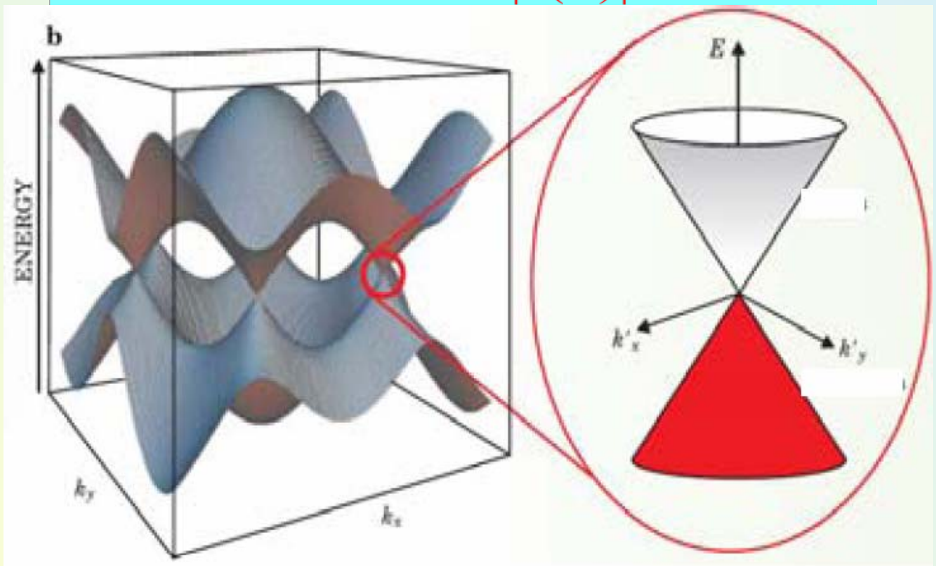

Electronic dispersion of a monolayer

Saito *et al*, "Physical Properties of Carbon Nanotubes" (Imperial College Press, London, 1998)

Symmetrical unit cell

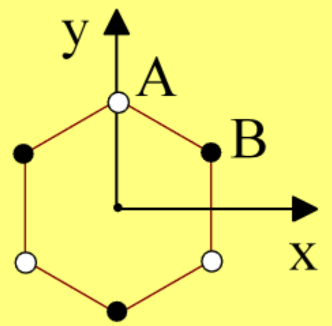

Two non-equivalent carbon positions

Brillouin zone

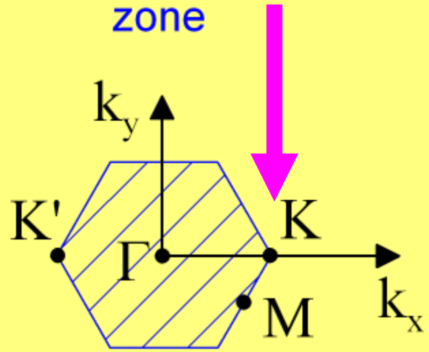

Two non-equivalent K-points

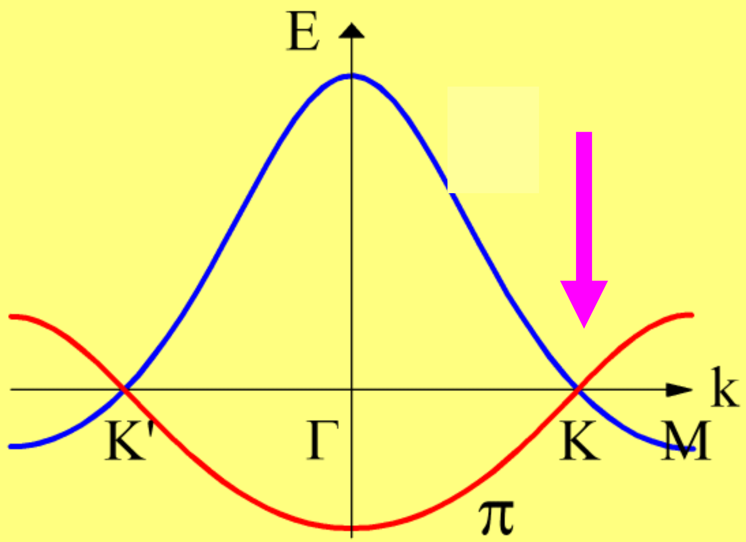

Two bands: no energy gap at the K-points

$$\Phi_j(\mathbf{k},\mathbf{r}) = \frac{1}{\sqrt{N}} \sum_{\mathbf{R}_j}^{N} e^{i\mathbf{k}.\mathbf{R}_j}\, \phi_j(\mathbf{r}-\mathbf{R}_j)$$

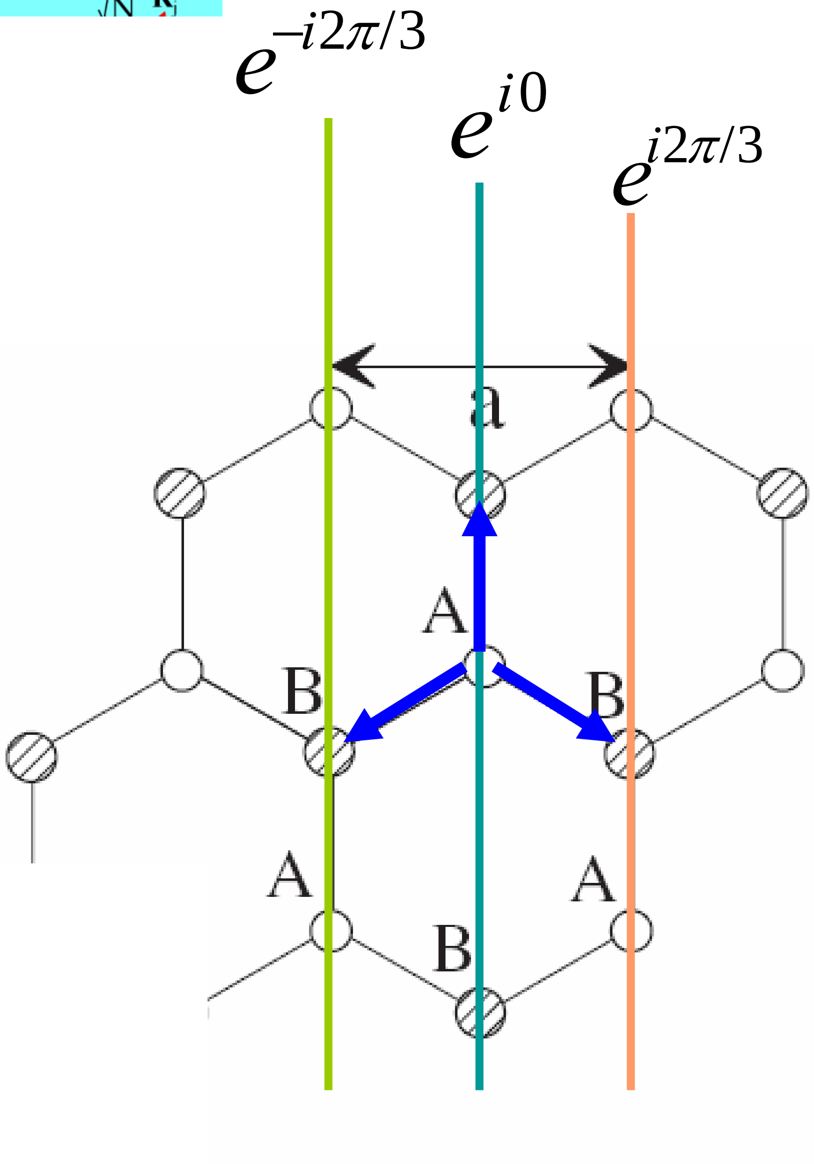

$$\Phi_j(\mathbf{k},\mathbf{r}) = \frac{1}{\sqrt{N}}\sum_{\mathbf{R}_j}^{N} e^{i\mathbf{k}.\mathbf{R}_j}\,\phi_j(\mathbf{r}-\mathbf{R}_j)$$

four-fold degeneracy

In the corners of the Brillouin zone, electron states on the A and B sub-lattices decouple and have exactly the same energy:

$$H_{AB} = -\gamma_0\left(e^{-i2\pi/3} + 1 + e^{i2\pi/3}\right) = 0$$

and also for both corners of the BZ,

$$\varepsilon(K_+) = \varepsilon(K_-) = 0$$

$$\begin{array}{l} A+ \\ B+ \\ B- \\ A- \end{array} \qquad \begin{pmatrix}1\\0\\0\\0\end{pmatrix};\begin{pmatrix}0\\1\\0\\0\end{pmatrix};\begin{pmatrix}0\\0\\1\\0\end{pmatrix};\begin{pmatrix}0\\0\\0\\1\end{pmatrix}$$

valley index

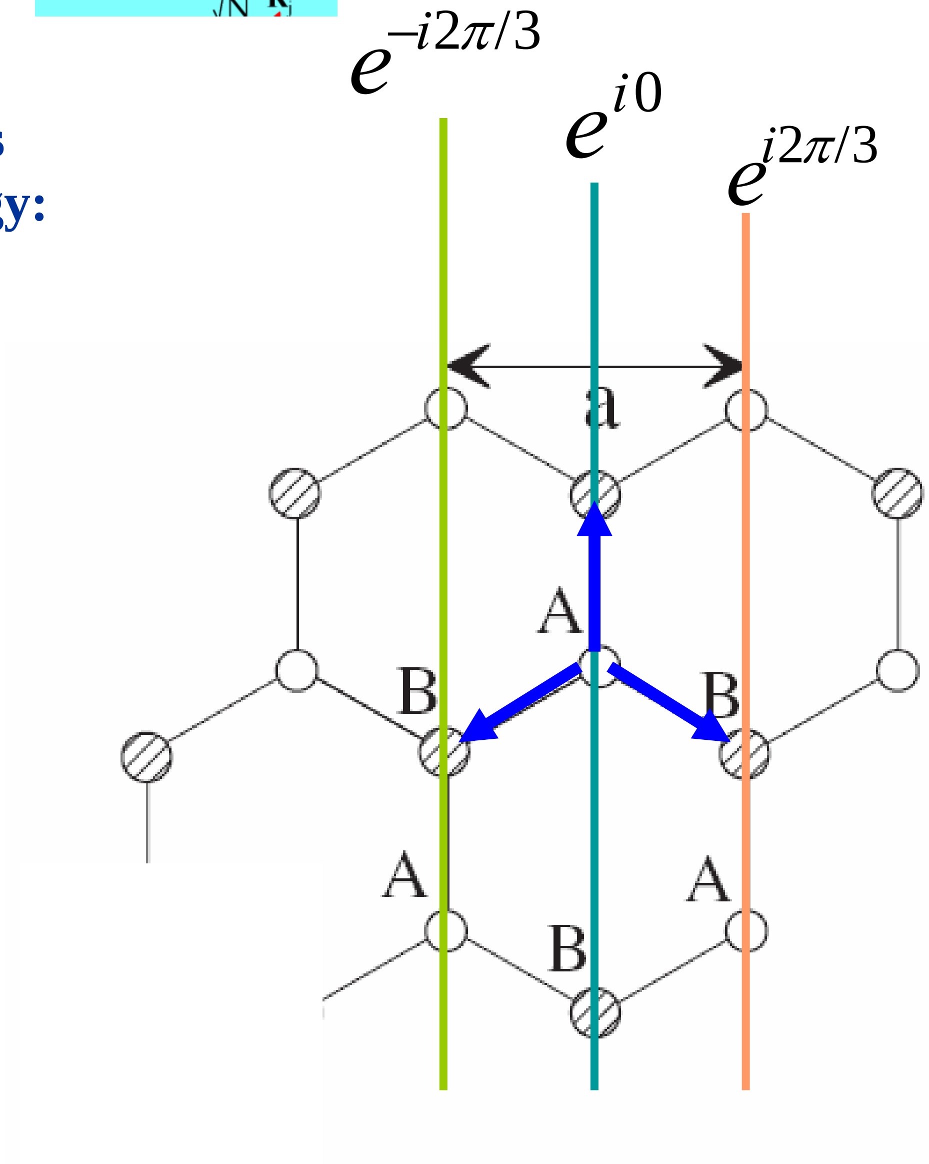

Four degenerate states in the corners of the Brillouin zone realize a 4-dimensional irreducible representation of the symmetry group of the honeycomb lattice

$$G\{C_{6v} \otimes T\}$$

$$\begin{array}{c} A+ \\ B+ \\ B- \\ A- \end{array} \quad \begin{pmatrix} 1 \\ 0 \\ 0 \\ 0 \end{pmatrix}; \begin{pmatrix} 0 \\ 1 \\ 0 \\ 0 \end{pmatrix}; \begin{pmatrix} 0 \\ 0 \\ 1 \\ 0 \end{pmatrix}; \begin{pmatrix} 0 \\ 0 \\ 0 \\ 1 \end{pmatrix}$$

Generating elements: $T_{A\to A}, C_{\frac{\pi}{3}}, S_x$

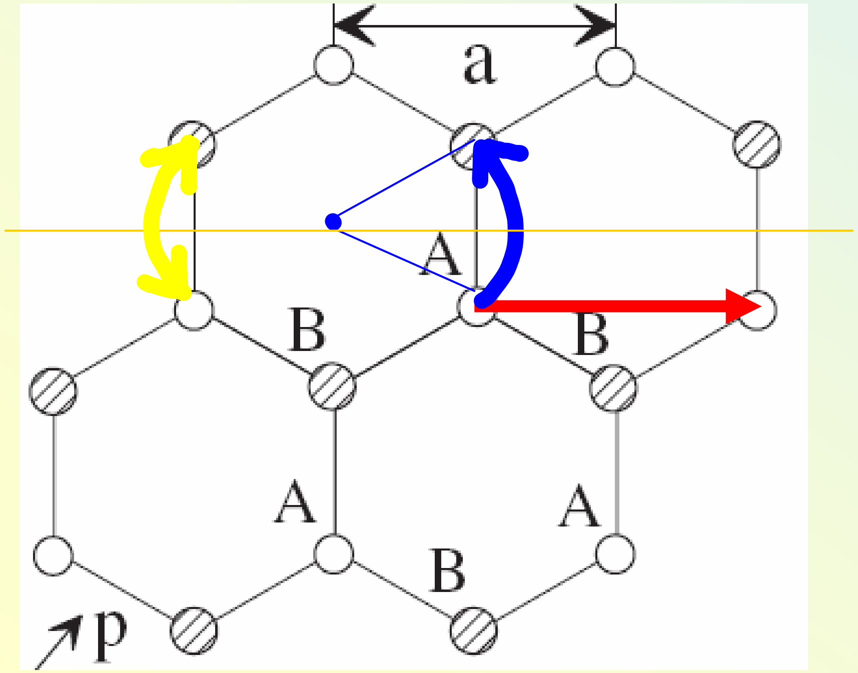

Translation $T_{A\to A}$

$$\begin{pmatrix} e^{i\frac{4\pi}{3}} & & & \\ & e^{i\frac{4\pi}{3}} & & \\ & & e^{-i\frac{4\pi}{3}} & \\ & & & e^{-i\frac{4\pi}{3}} \end{pmatrix}$$

Rotation $C_{\frac{\pi}{3}}$

$A \longleftrightarrow B$

$K_+ \longleftrightarrow K_-$

$$\begin{pmatrix} & & e^{i\frac{2\pi}{3}} & \\ & & & e^{-i\frac{2\pi}{3}} \\ e^{i\frac{2\pi}{3}} & & & \\ & e^{-i\frac{2\pi}{3}} & & \end{pmatrix}$$

Mirror reflection S_x

$A \longleftrightarrow B$

$$\begin{pmatrix} & 1 & & \\ 1 & & & \\ & & & 1 \\ & & 1 & \end{pmatrix}$$

Brillouin zone

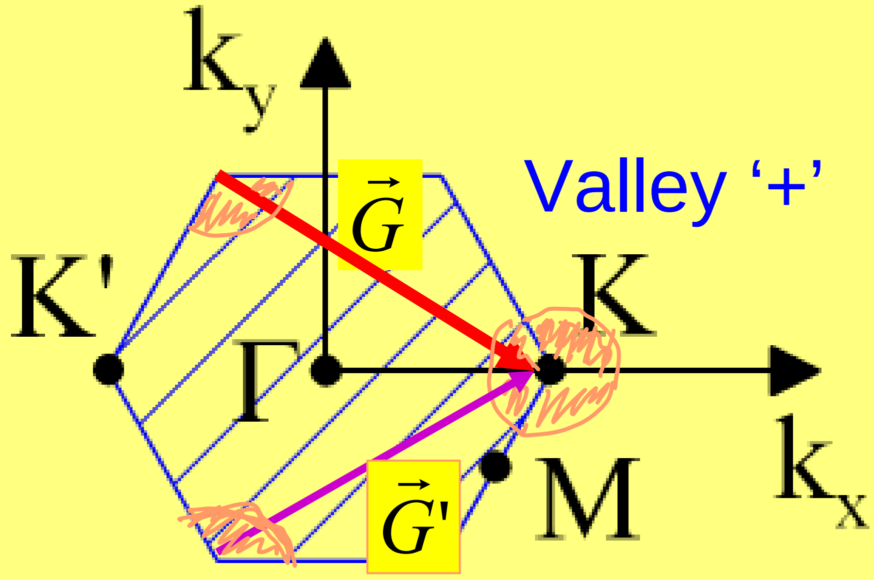

Two non-equivalent K-points

$$H_{AB,K_+} = -\gamma_0 \left[e^{-i\frac{2\pi}{3}} e^{-i(\frac{a}{2}p_x + \frac{a}{2\sqrt{3}}p_y)} + e^{i\frac{a}{\sqrt{3}}p_y} + e^{i\frac{2\pi}{3}} e^{i(\frac{a}{2}p_x - \frac{a}{2\sqrt{3}}p_y)} \right]$$

$$\approx -\frac{\sqrt{3}}{2}\gamma_0 a(p_x - ip_y) = -\frac{\sqrt{3}}{2}\gamma_0 a\pi^+$$

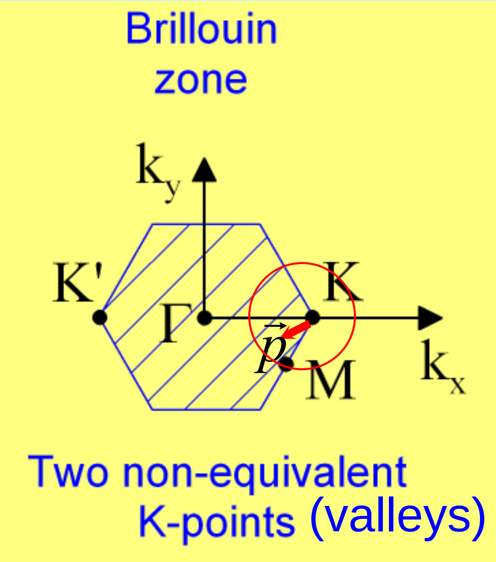

$$\pi^+ = p_x - ip_y$$

$$\pi = p_x + ip_y$$

$$H_{BA,K_+} \approx -\frac{\sqrt{3}}{2}\gamma_0 a(p_x + ip_y) = -\frac{\sqrt{3}}{2}\gamma_0 a\pi$$

$$v = \frac{\sqrt{3}}{2}\gamma_0 a \sim 10^8 \frac{cm}{\sec}$$

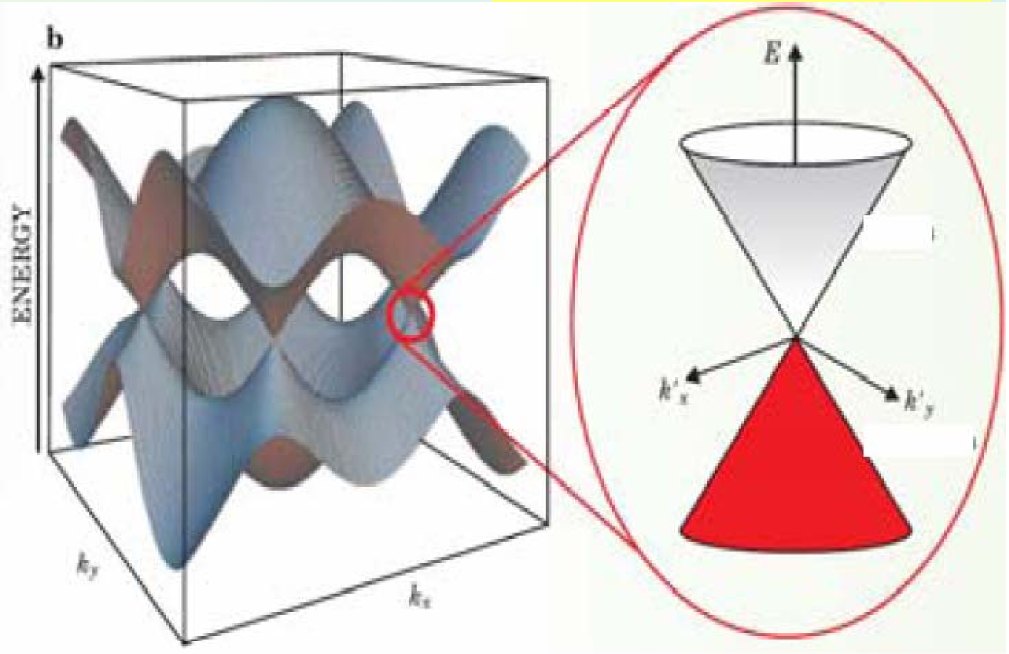

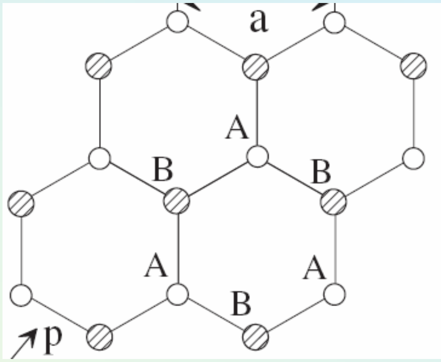

valley index
'pseudospin'

$$\hat{H} = \begin{pmatrix} 0 & \pi^+ & & \\ \pi & 0 & & \\ & & 0 & -\pi^+ \\ & & -\pi & 0 \end{pmatrix} \begin{pmatrix} \varphi_{A,+} \\ \varphi_{B+} \\ \varphi_{B-} \\ \varphi_{A-} \end{pmatrix}$$

sublattice index
'isospin'

$$\pi = p_x + ip_y$$

$$\pi^+ = p_x - ip_y$$

Brillouin
zone

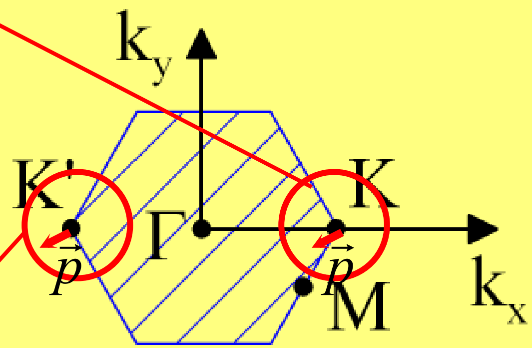

Two non-equivalent
K-points

Also, one may need to take into account an additional real spin degeneracy of all states

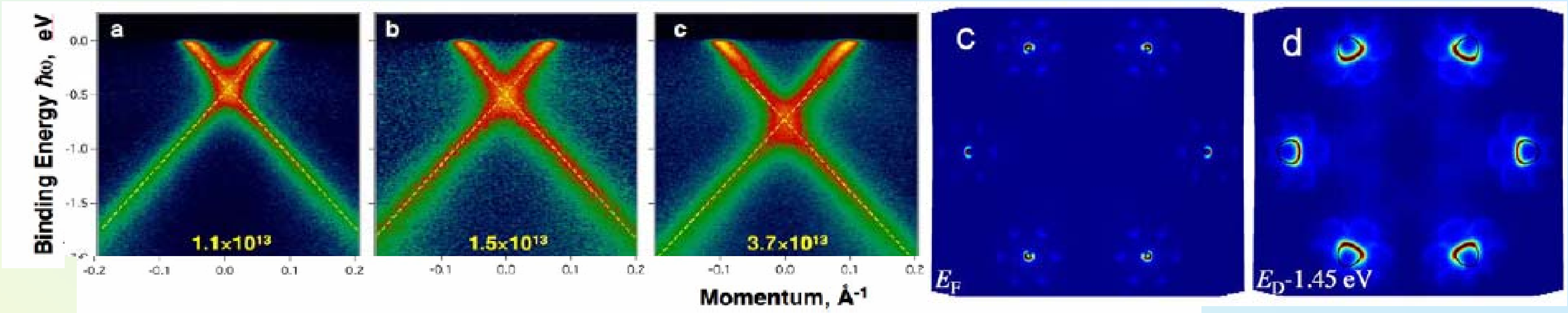

ARPES: heavily doped graphene synthesized on silicon carbide

A. Bostwick *et al* – Nature Physics, 3, 36 (2007)

Dirac Hamiltonian of a monolayer

written in a 2 component basis of A and B sites

B to A hopping given by $\pi^+ = p_x - ip_y$

$$\boxed{H = v\xi \begin{pmatrix} 0 & \pi^+ \\ \pi & 0 \end{pmatrix} = v\xi(\sigma_x p_x + \sigma_y p_y)}$$

A to B hopping given by $\pi = p_x + ip_y$

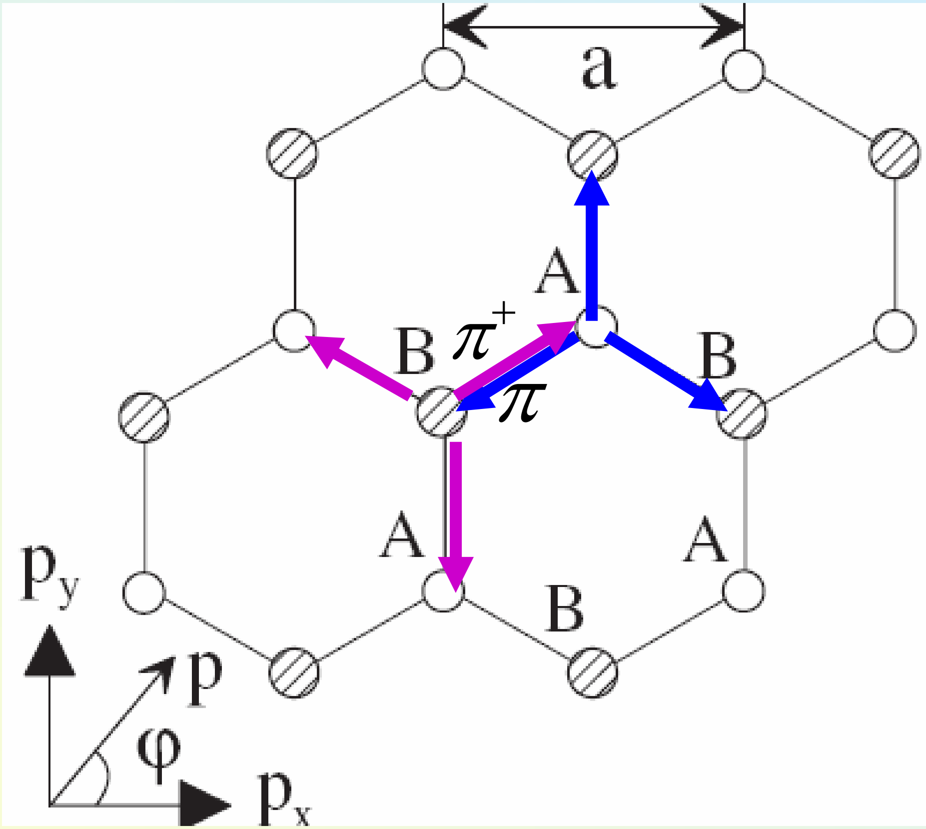

Monolayer graphene

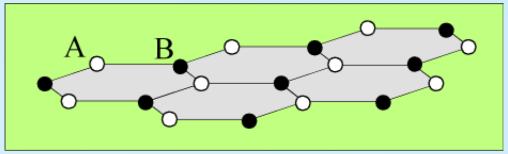

Lattice, symmetry and band structure of monolayer graphene.

Intricate details: trigonal warping in the band structure.

'Chiral' electrons and Berry's phase π in monolayer graphene,
suppressed backscattering of chiral electrons.

Unusual properties of the PN junction in graphene
focusing & caustics, Veselago lens for electrons.

To write down the monolayer Hamiltonian describing electrons near the K-points, one has to construct all possible invariants using 4x4 matrices (with sublattice and valley indices) acting within the 4-dimensional representation and the momentum operator, $\vec{p}$.
(phenomenology)

Alternatively, one can apply the tight-binding model including the dominant next-neighbour (AB) hop and also longer-distance (AA) hops
and to expand to higher order in $pa << 1$ (or π, π^+).
(microscopy)

$$H_{AB,K_+} = -\gamma_0 \left[e^{-i\frac{2\pi}{3}} e^{-i\left(\frac{a}{2}p_x + \frac{a}{2\sqrt{3}}p_y\right)} + e^{i\frac{a}{\sqrt{3}}p_y} + e^{i\frac{2\pi}{3}} e^{i\left(\frac{a}{2}p_x - \frac{a}{2\sqrt{3}}p_y\right)} \right]$$

$$\approx \frac{\sqrt{3}}{2}\gamma_0 a(p_x - ip_y) - \frac{\gamma_0 a^2}{8}(p_x + ip_y)^2$$

higher order invariants (expansion terms)

$$\hat{H} = \varsigma v \begin{pmatrix} 0 & \pi^+ \\ \pi & 0 \end{pmatrix} + \mu \begin{pmatrix} 0 & \pi^2 \\ (\pi^+)^2 & 0 \end{pmatrix} + \delta \cancel{\begin{pmatrix} p^2 & 0 \\ 0 & p^2 \end{pmatrix}}$$

$$\begin{pmatrix} A,+ \\ B,+ \\ B,- \\ A,- \end{pmatrix}$$

valley

$\varsigma = \pm 1$

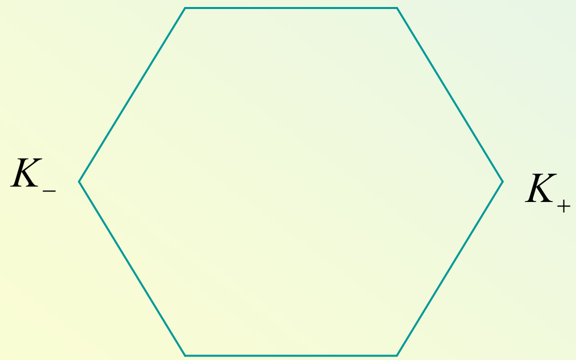

~~**a weak electron-hole asymmetry due to non-orthogonality of orbital basis and AA, BB hopping**~~

$$\hat{H} = \varsigma v \begin{pmatrix} 0 & \pi^+ \\ \pi & 0 \end{pmatrix} + \mu \begin{pmatrix} 0 & \pi^2 \\ (\pi^+)^2 & 0 \end{pmatrix}$$

weak 'trigonal warping': which has interesting consequences for the weak localisation effect (Lecture 3).

valley

$\varsigma = \pm 1$

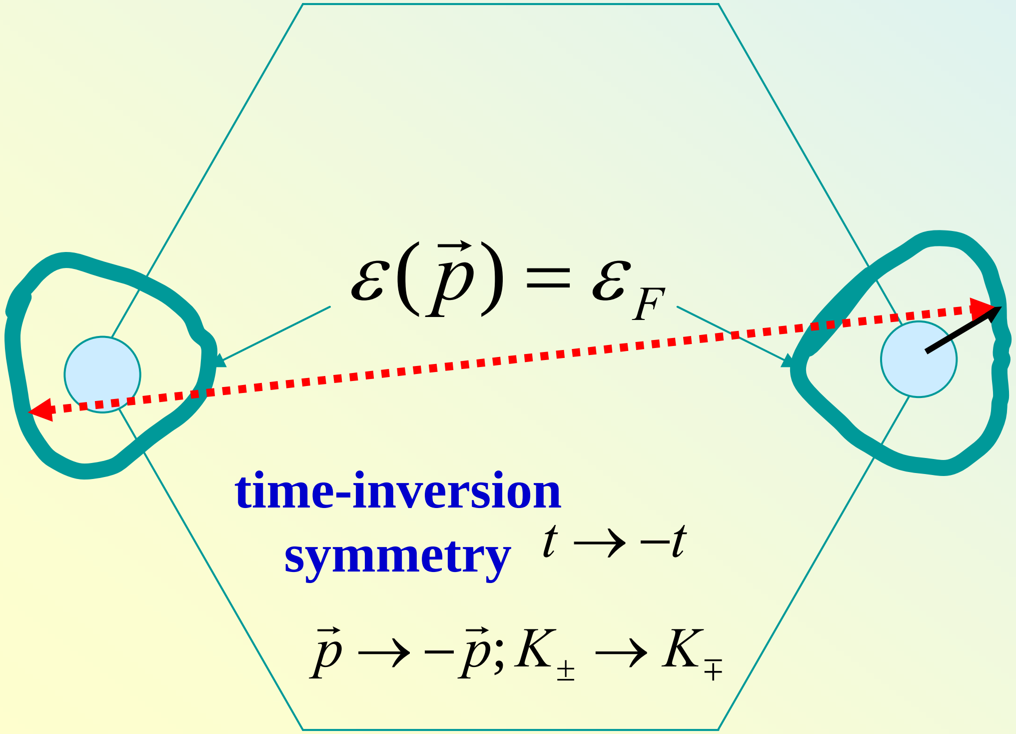

$$\pi = p_x + ip_y = pe^{i\varphi}$$

$$\pi = p_x - ip_y = pe^{-i\varphi}$$

$$\vec{p} = p(\cos\varphi, \sin\varphi)$$

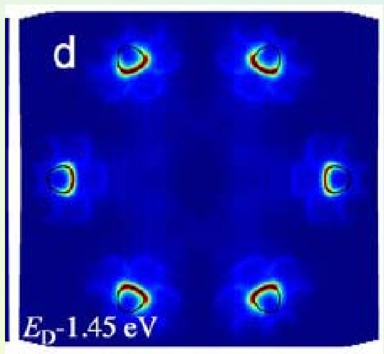

A. Bostwick *et al* – Nature Physics, 3, 36 (2007)

Monolayer graphene

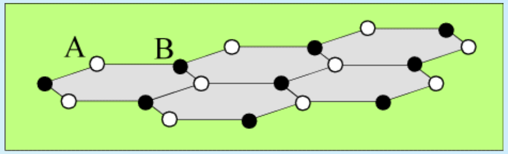

Lattice, symmetry and band structure of monolayer graphene.

Intricate details: trigonal warping in the band structure.

'Chiral' electrons and Berry's phase π in monolayer graphene,
suppressed backscattering of chiral electrons.

Unusual properties of the PN junction in graphene
focusing & caustics, Veselago lens for electrons.

Monolayer graphene: truly two-dimensional gapless semiconductor with the Dirac-type spectrum of electrons

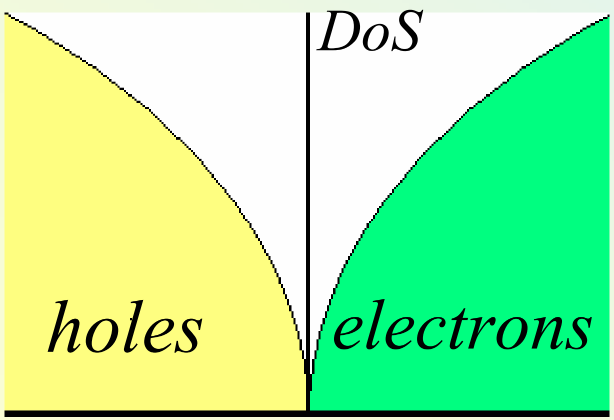

$$n_{carriers} \propto V_{gate}$$

Wallace, Phys. Rev. 71, 622 (1947)

Monolayer

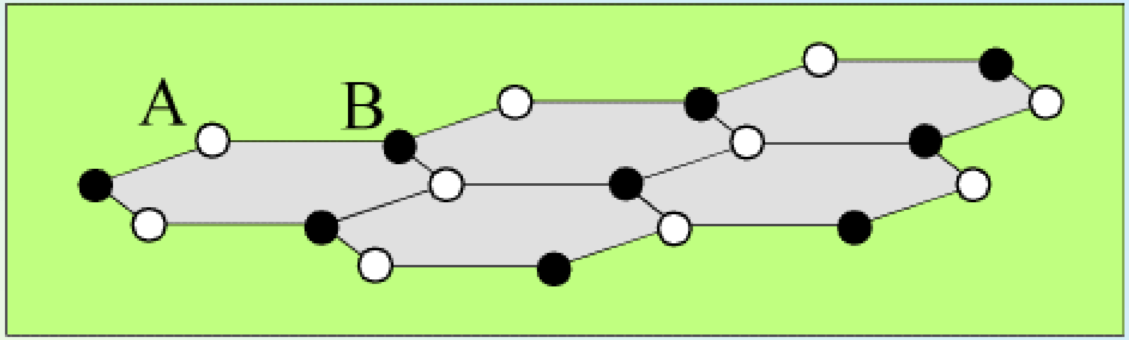

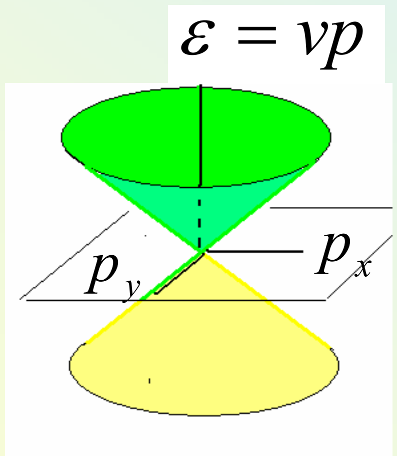

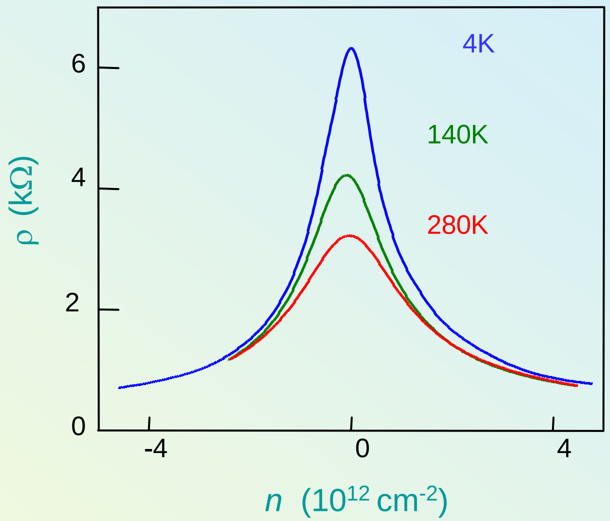

K. Novoselov et al., Science 306, 666 (2004)

Bloch function amplitudes (e.g., in the valley K) on the AB sites ('isospin') mimic spin components of a relativistic Dirac fermion.

$$\pi^{+} = p_x - ip_y$$

$$\pi = p_x + ip_y$$

$$\psi = \begin{pmatrix} \varphi_A \\ \varphi_B \end{pmatrix}$$

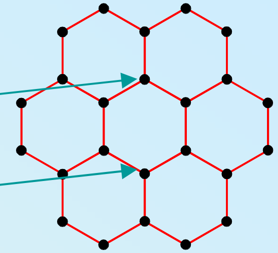

$$H_1 = v\begin{pmatrix} 0 & \pi^{+} \\ \pi & 0 \end{pmatrix} = v\vec{\sigma}\cdot\vec{p} = vp\ \vec{\sigma}\cdot\vec{n}$$

Chiral electrons

isospin direction is linked to the axis determined by the electron momentum.

$$\varepsilon = vp$$

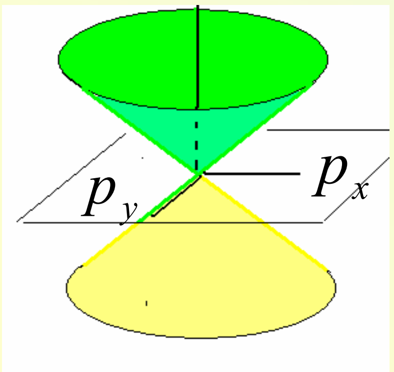

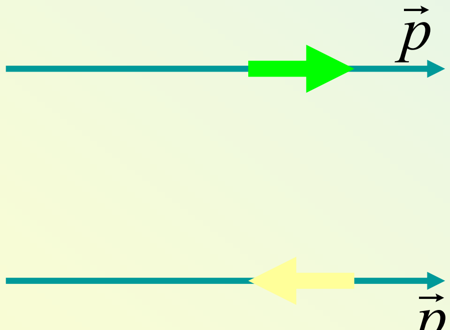

for conduction band electrons,

$$\vec{\sigma}\cdot\vec{n} = 1$$

$$\vec{\sigma}\cdot\vec{n} = -1$$

valence band ('holes')

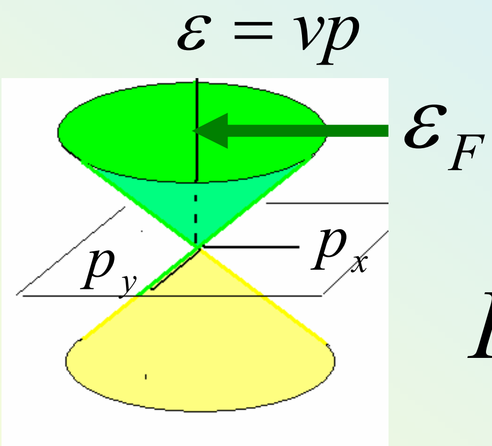

$$\hat{H}_1 = v\begin{pmatrix} 0 & \pi^+ \\ \pi & 0 \end{pmatrix} = v\vec{\sigma}\cdot\vec{p} = vp\ \vec{\sigma}\cdot\vec{n}$$

Bloch function amplitudes on the AB sites - ‘isospin’

$$\psi = \begin{pmatrix} \varphi_A \\ \varphi_B \end{pmatrix}$$

Chiral electrons:

‘isospin’ direction is linked to the axis determined by the electron momentum,

$$\vec{\sigma}\cdot\vec{n} = 1$$

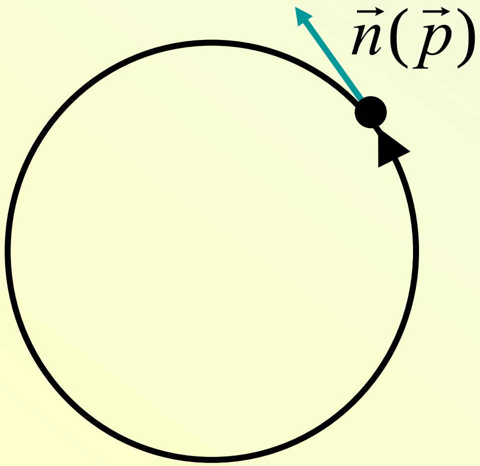

$$\psi \rightarrow e^{2\pi\frac{i}{2}\sigma_3}\psi = e^{i\pi}\psi$$

Berry phase π

$$H_1 = v\begin{pmatrix} 0 & \pi^+ \\ \pi & 0 \end{pmatrix} = v\vec{\sigma}\cdot\vec{p} = vp\ \vec{\sigma}\cdot\vec{n}$$

$$\pi = p_x + ip_y = pe^{i\varphi}$$
$$\pi^+ = p_x - ip_y = pe^{-i\varphi}$$

Chiral electrons: isospin direction is linked to the electron momentum.

$$\varepsilon = vp$$

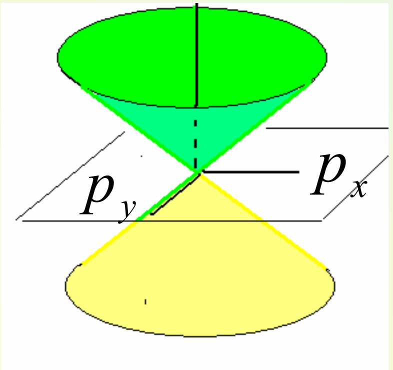

$$\psi_{\vec{p}} = \tfrac{1}{\sqrt{2}}\begin{pmatrix} e^{i\theta/2} \\ e^{-i\theta/2} \end{pmatrix}$$

for conduction band electrons,

$\vec{\sigma}\cdot\vec{n} = 1$ $\quad \vec{p}$

$\vec{\sigma}\cdot\vec{n} = -1$ $\quad \vec{p}$

valence band

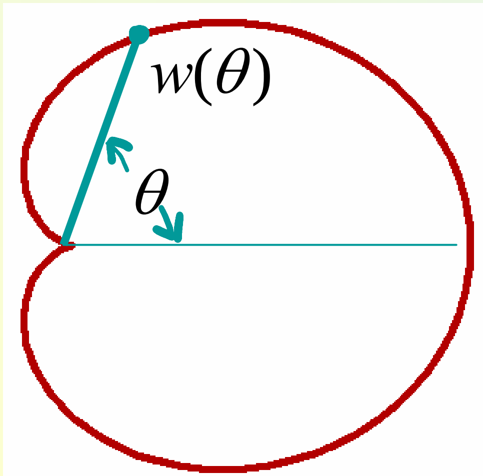

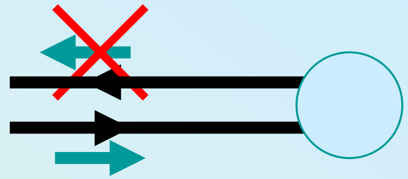

$$\vec{\sigma}\cdot\vec{n} = 1$$

Due to the isospin conservation, A-B symmetric potential cannot backward scatter chiral fermions,

Ando, Nakanishi, Saito
J. Phys. Soc. Jpn 67, 2857 (1998)

$$w(\theta) \sim \cos^2\tfrac{\theta}{2}\, f(|\vec{p}-\vec{p}'|)$$

Monolayer graphene

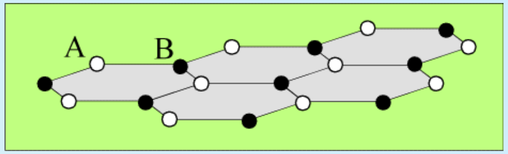

Lattice, symmetry and band structure of monolayer graphene.

Intricate details: trigonal warping in the band structure.

'Chiral' electrons and Berry's phase π in monolayer graphene,
suppressed backscattering of chiral electrons.

Unusual properties of the PN junction in graphene
focusing & caustics, Veselago lens for electrons.

PN junctions in the usual gap-full semiconductors are non-transparent for incident electrons, therefore, they are highly resistive.

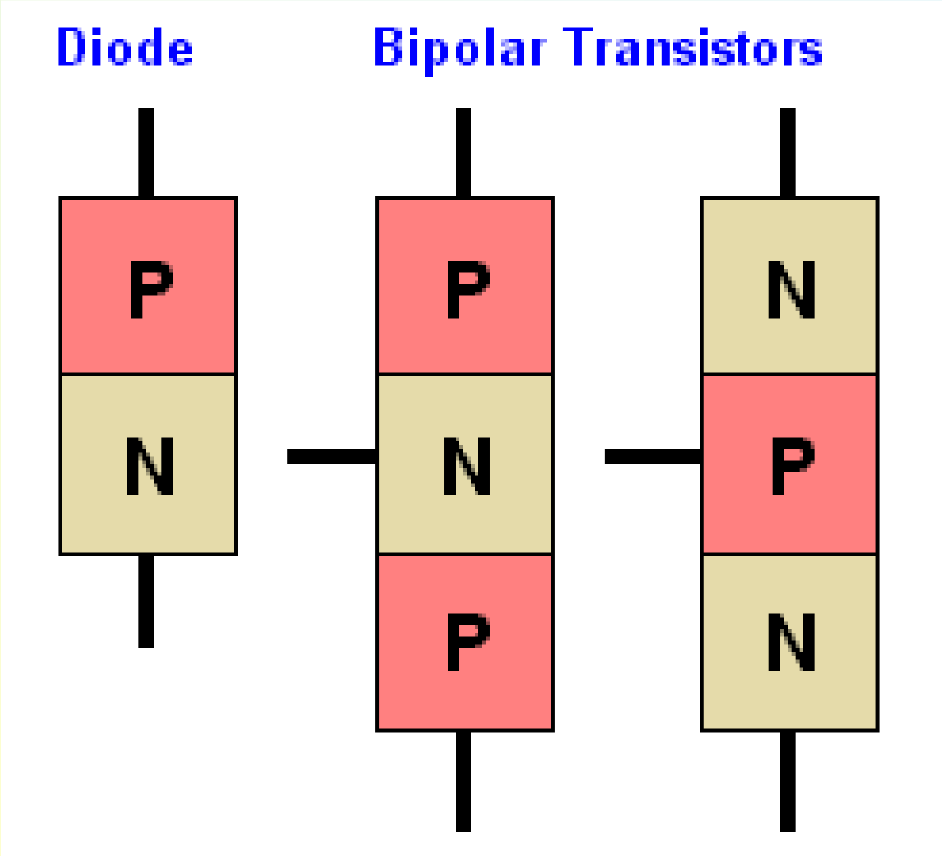

Transmission of chiral electrons through the PN junction in graphene

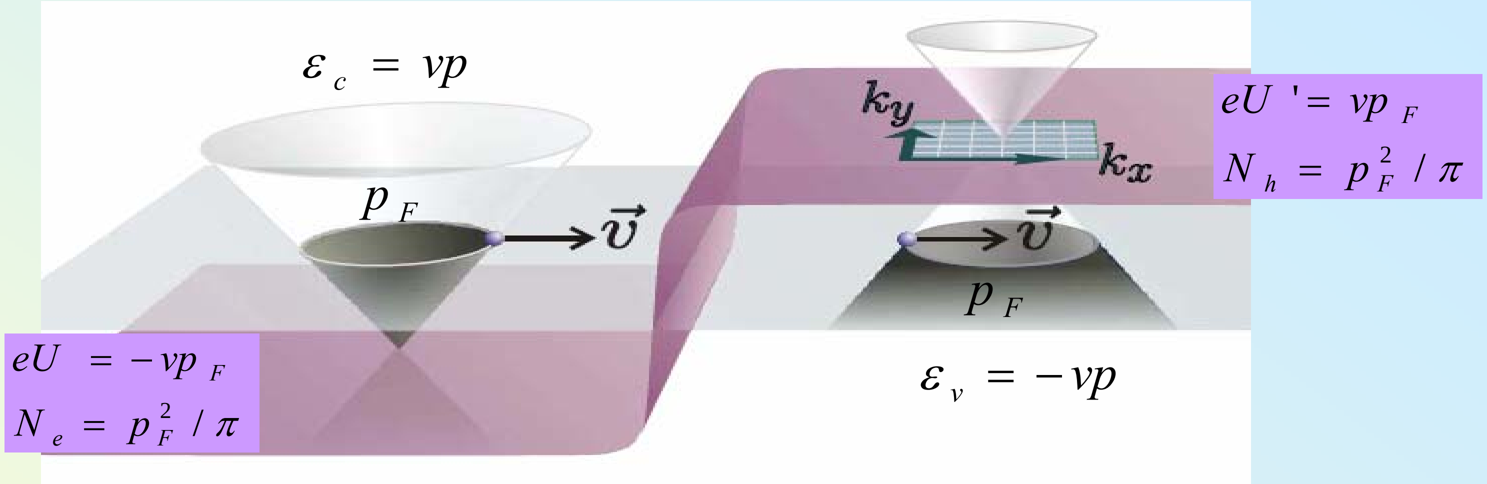

conduction band electrons

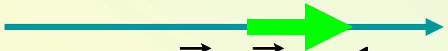

$\vec{p}$

$$\vec{\sigma}\cdot\vec{n} = 1$$

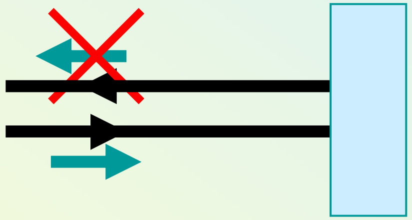

$$\psi_{\vec{p}} = \frac{1}{\sqrt{2}}\begin{pmatrix} e^{i\theta/2} \\ e^{-i\theta/2} \end{pmatrix}$$

Due to the isospin conservation, A-B symmetric potential cannot backward scatter chiral electrons

$$\hat{H} = v\vec{\sigma}\cdot\vec{p}$$

For graphene PN junctions: Cheianov, VF - PR B 74, 041403 (2006)

'Klein paradox': Katsnelson, Novoselov, Geim, Nature Physics 2, 620 (2006)

Transmission of chiral electrons through the PN junction in graphene

$$\sqrt{p_x^2 + p_F^2 \sin^2\theta} + U(x) = \mu$$

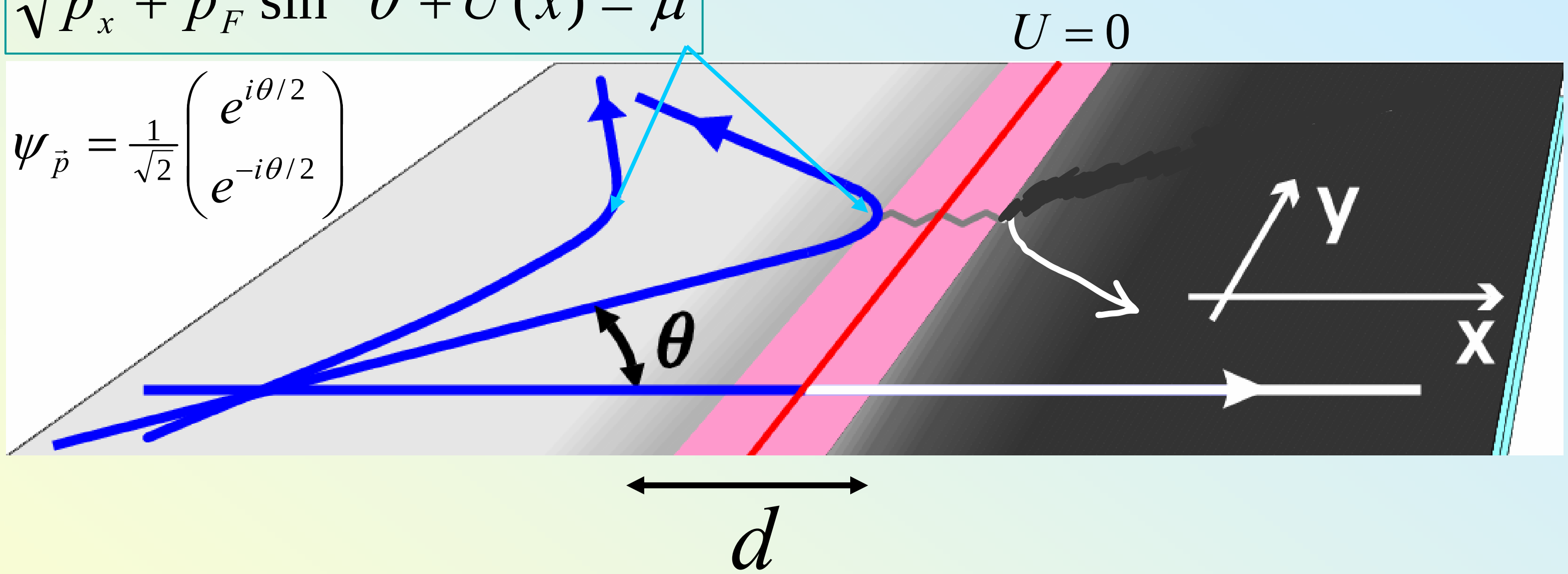

Due to the 'isospin' conservation, electrostatic potential ***U(x)*** which smooth on atomic distances cannot scatter chiral fermions in the exactly backward direction.

$$w(\theta) = e^{-\pi p_F d \sin^2\theta} \cos^2\theta$$

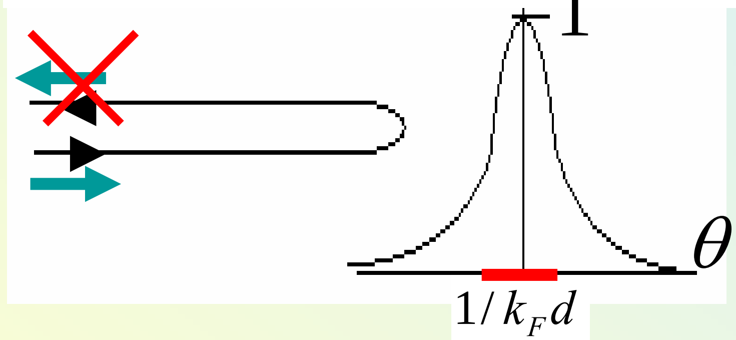

Transmission of chiral electrons through the PN junction in graphene

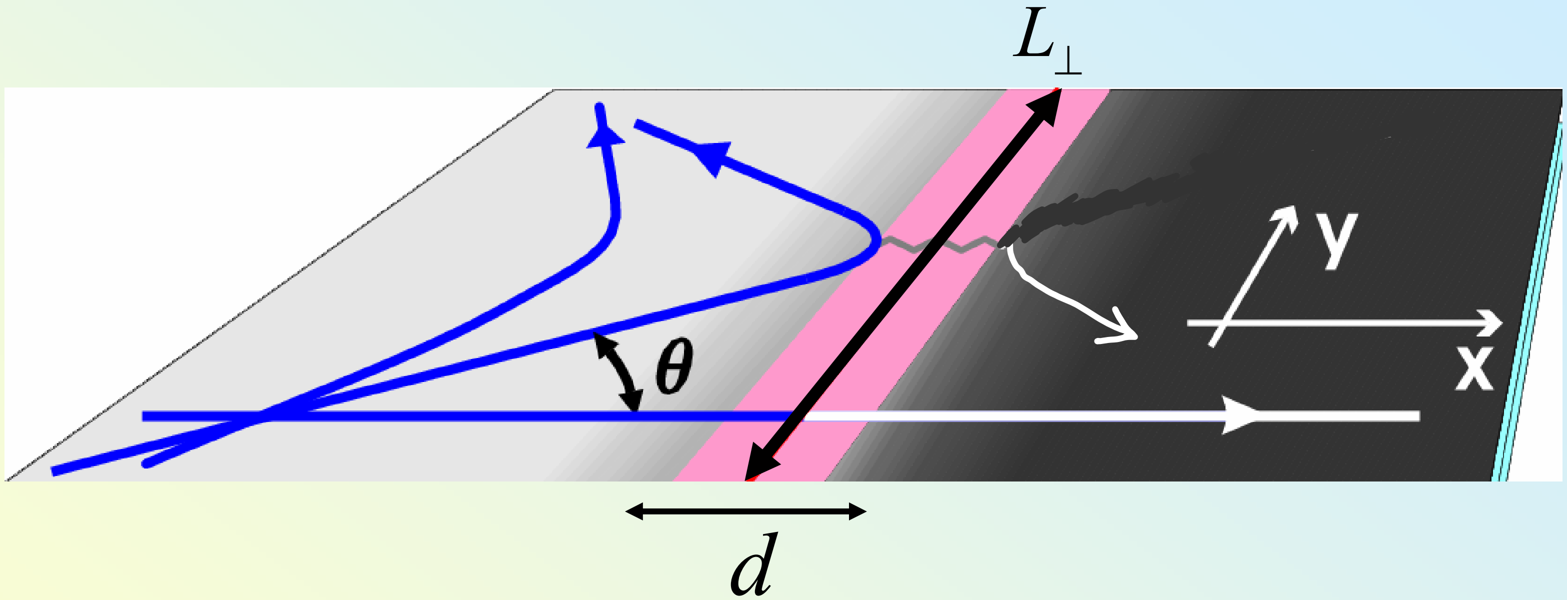

Due to transmission of electrons with a small incidence angle, $\theta<1/p_F d$, a PN junction in graphene should display a finite conductance (no pinch-off)

$$\boxed{\frac{g_{np}}{L_\perp} = \frac{2e^2}{\pi h}\sqrt{\frac{p_F}{d}}}$$

A characteristic Fano factor in the shot noise:

$$\langle I \cdot I \rangle = (1-\sqrt{\tfrac{1}{2}})\ eI$$

Cheianov, VF - PR B 74, 041403 (2006)

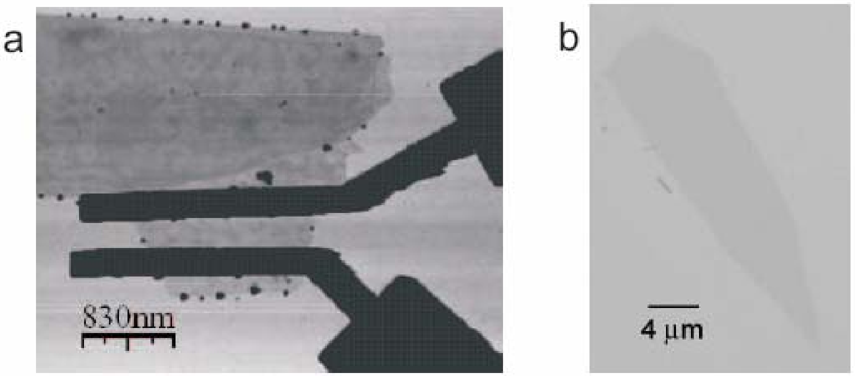

Fig. 2. (a) Atomic force microscopy image of a single-layer graphene Josephson junction used in our experiments. The electrodes consist of a Ti/Al bilayer, with the Tutatnium in contact with graphen.(b) Large graphene layer deposited on top of a Si/SiO_2 substrate by controlled exfoliation of a single graphite crystal. graphe

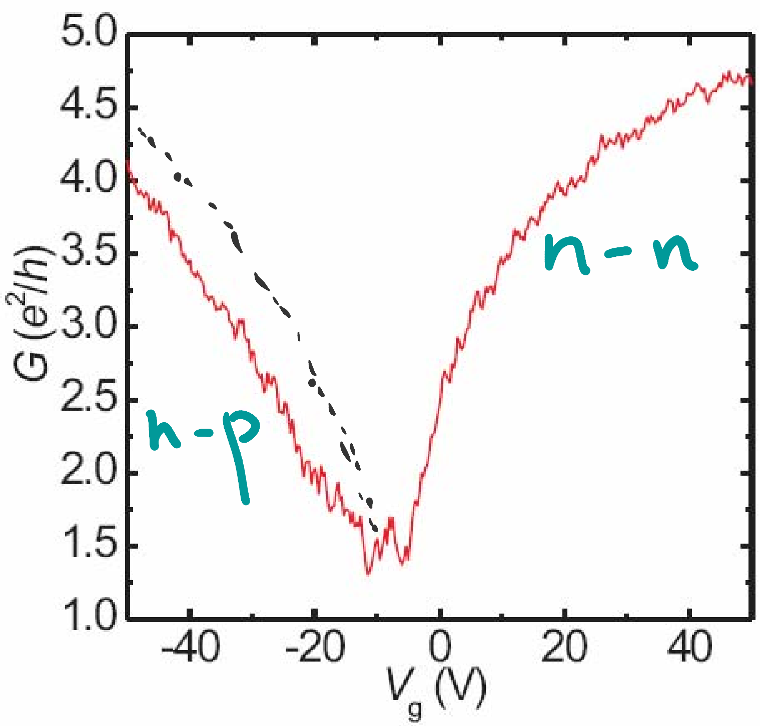

PN junctions should be taken into consideration in two-terminal devices, since contacts dope graphene.

Heersche *et al* - Nature Physics (2007)

Wishful thinking about graphene microstructures

Focusing and Veselago lens for electrons in ballistic graphene

Cheianov, VF, Altshuler - Science 315, 1252 (2007)

$$\varepsilon_c(\vec{p}) = vp$$

$$\vec{v} = \frac{\partial \varepsilon}{\partial \vec{p}} = v\frac{\vec{p}}{p}$$

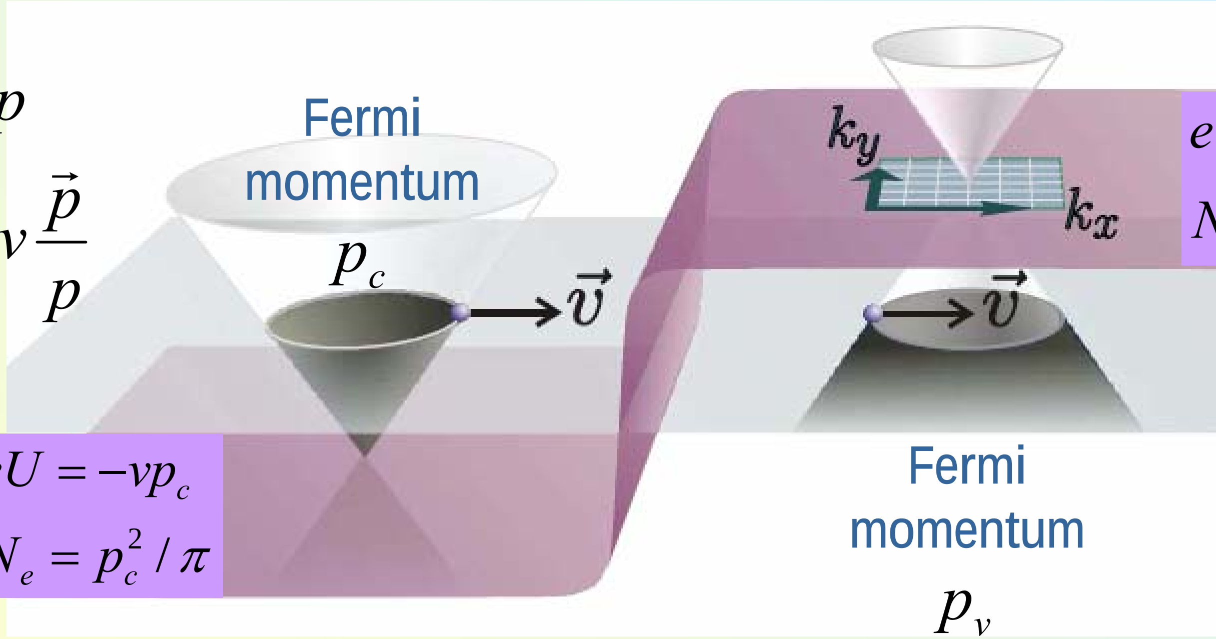

$$eU = -vp_c$$

$$N_e = p_c^2/\pi$$

$$eU' = vp_v$$

$$N_h = p_v^2/\pi$$

$$\varepsilon_v(\vec{p}) = -vp$$

$$\vec{v} = \frac{\partial \varepsilon}{\partial \vec{p}} = -v\frac{\vec{p}}{p}$$

The effect we'll discuss would be the strongest in sharp PN junction, with $d \sim \lambda_F$.

PN junction

$$p_y = p_y^{'} \Rightarrow p_c \sin\theta_c = -p_v \sin\theta_v$$

$$\boxed{\frac{\sin\theta_c}{\sin\theta_v} = -\frac{k_v}{k_c} = n}$$

Snell's law with negative refraction index

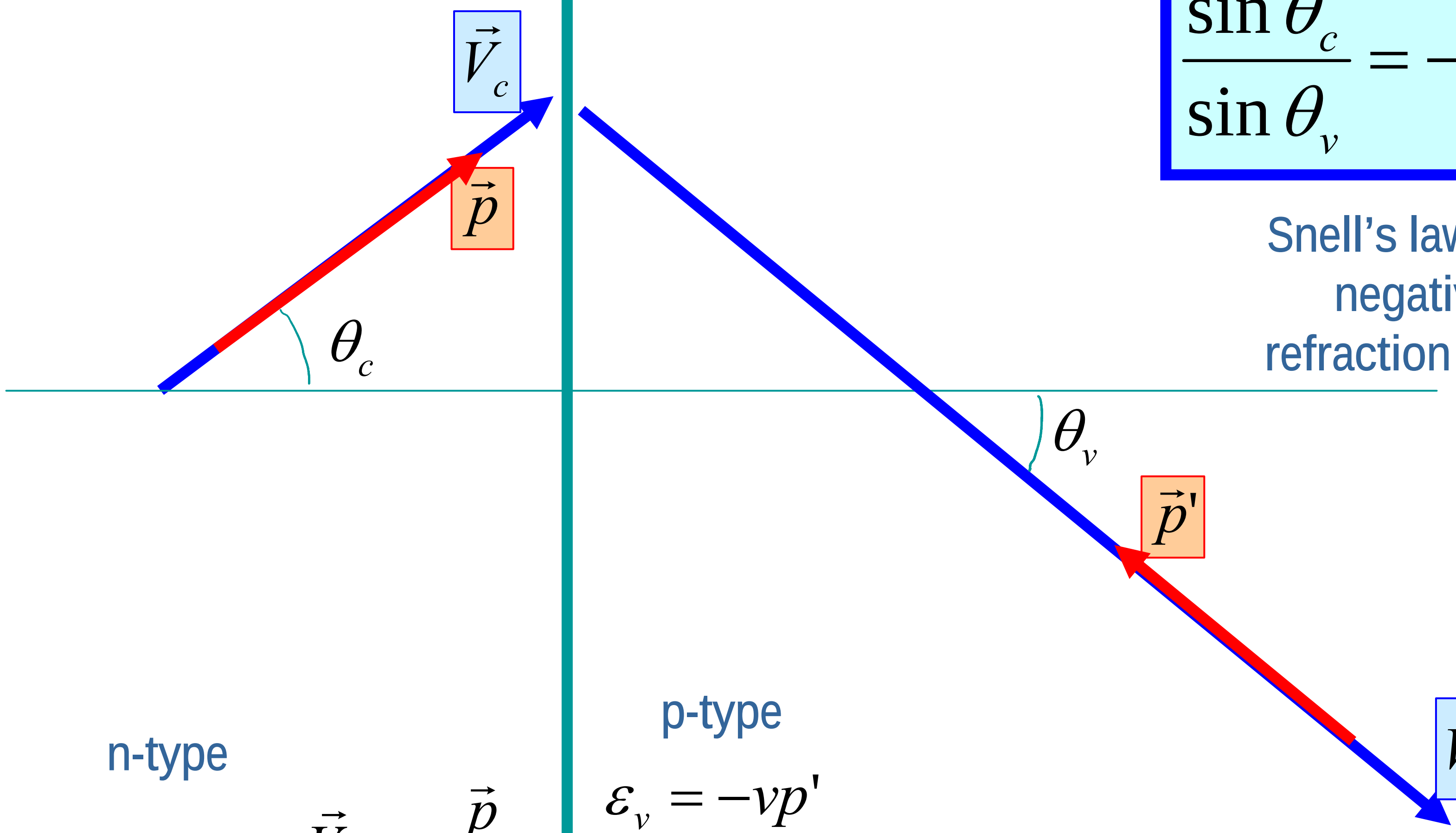

n-type

$$\varepsilon_c = vp; \quad \vec{V}_c = v\frac{\vec{p}}{p}$$

p-type

$$\varepsilon_v = -vp'$$

$$\vec{V}_v = -v\frac{\vec{p}'}{p'}$$

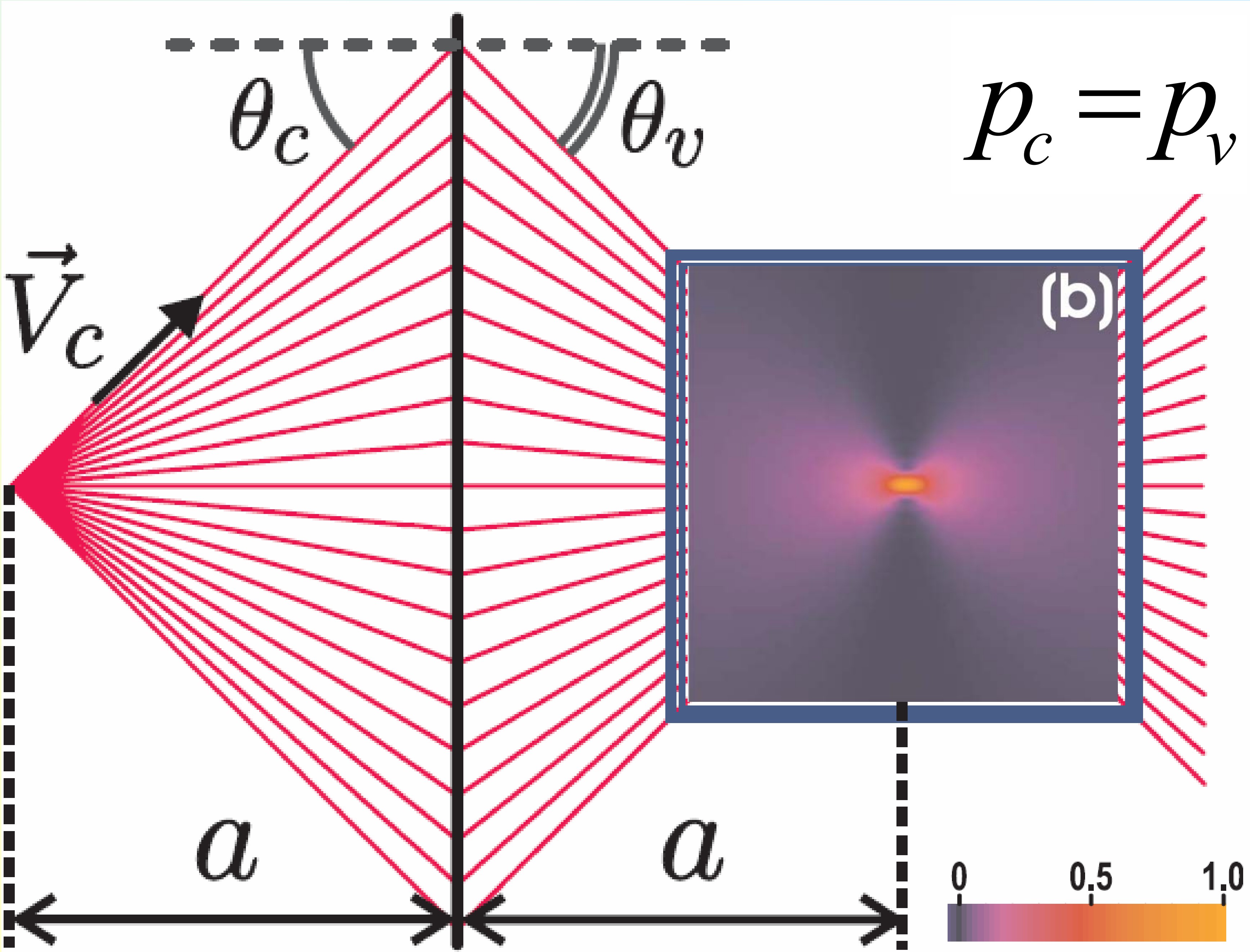

θ_c
θ_v
$p_c = p_v$
$\vec{V}_c$
(b)
a
a
0
0.5
1.0

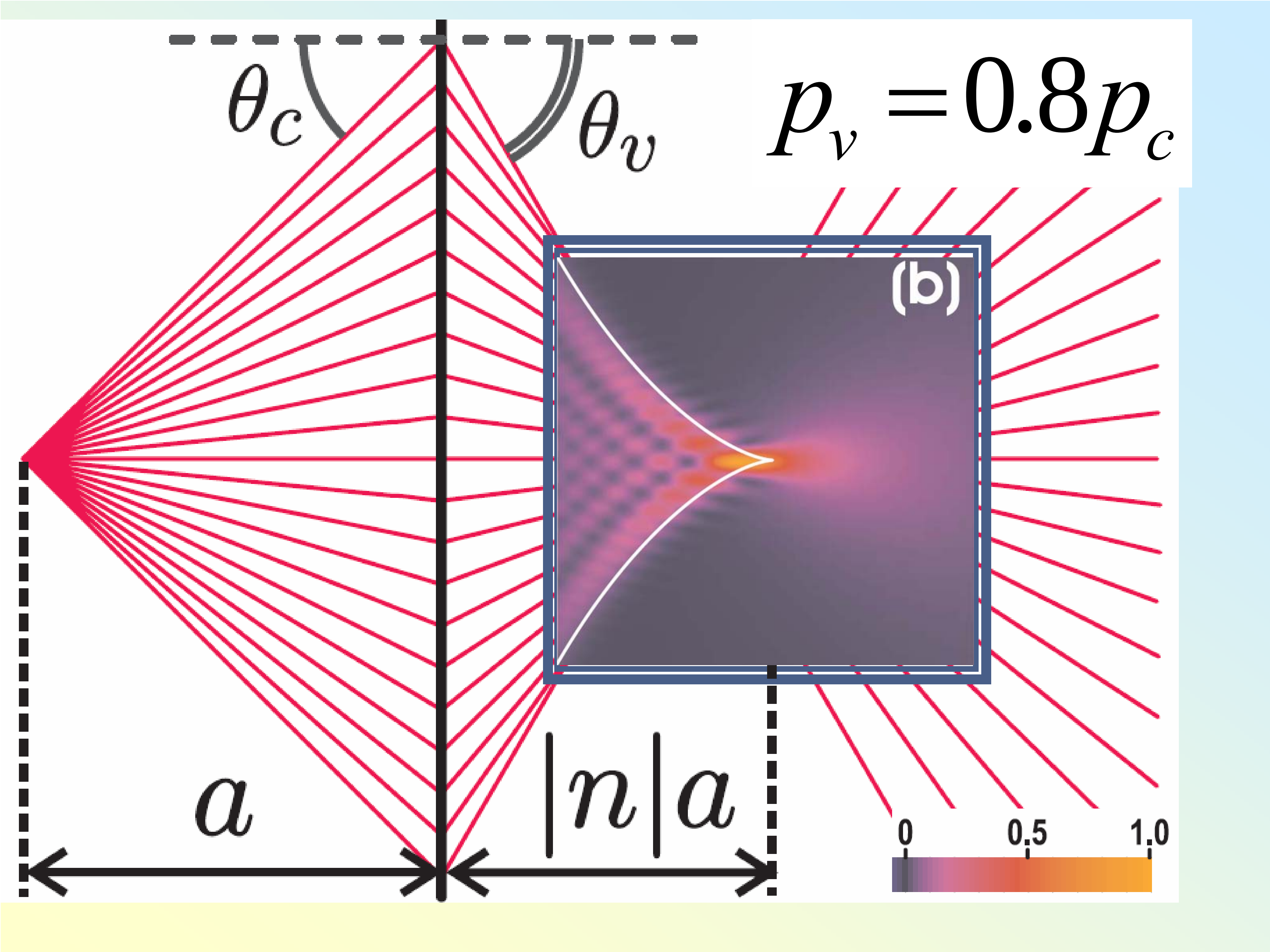

θ_c
θ_v
$p_v = 0.8 p_c$
(b)
a
$|n|a$
0
0.5
1.0

Veselago Lens for photons

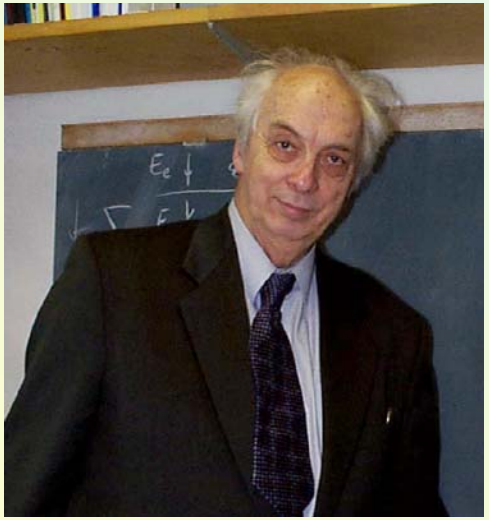

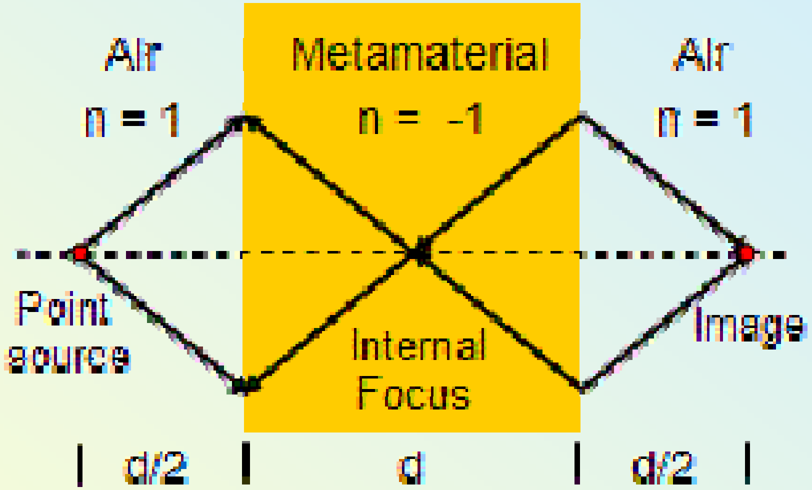

Veselago, Sov. Phys.-Usp., 10, 509 (1968)

Pendry, Phys. Rev. Lett., 85, 3966 (2000)

Graphene bipolar transistor: Veselago lens for electrons

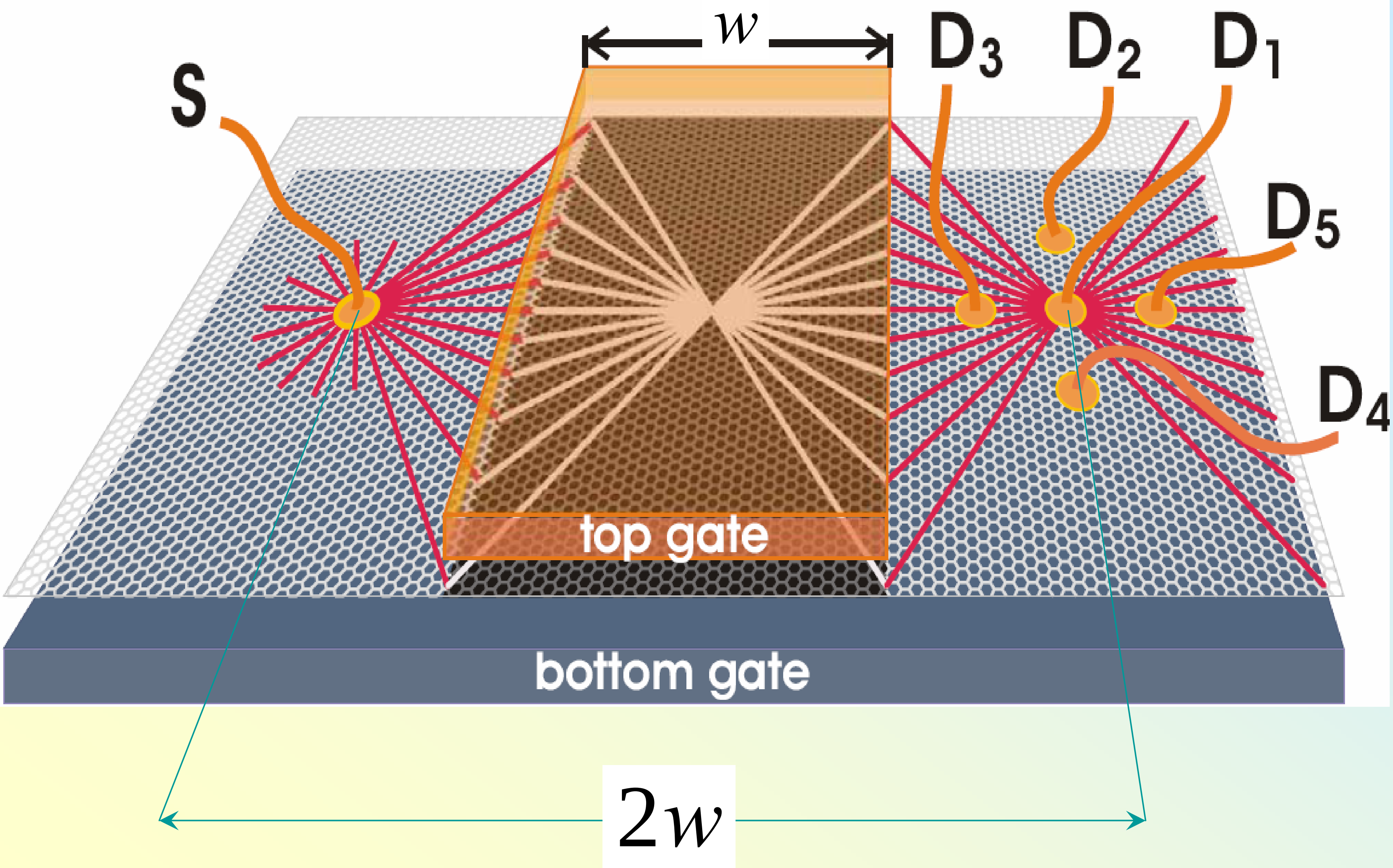

Focusing prism (beam-splitter) for electrons

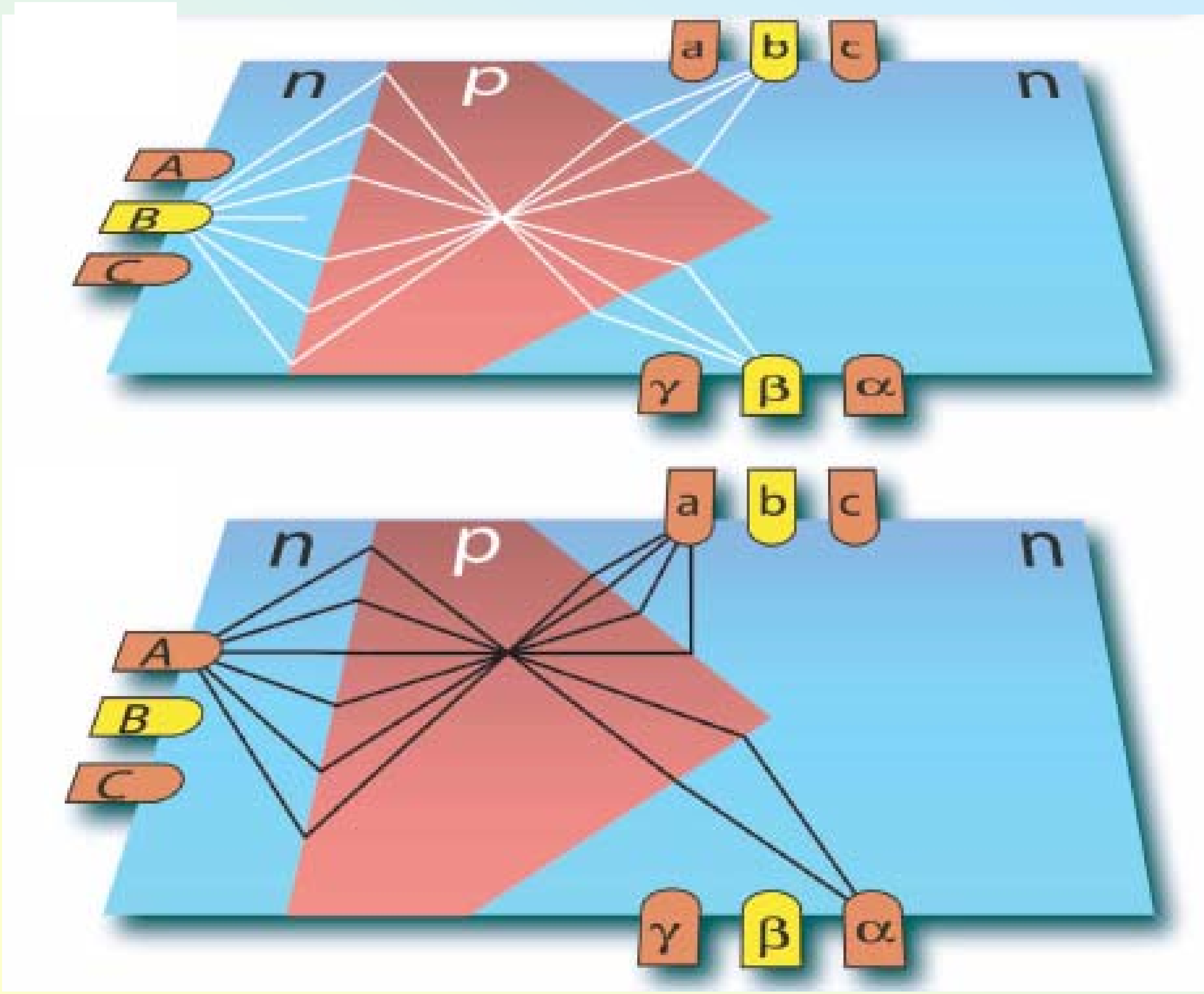

Graphite

studied from 1930th

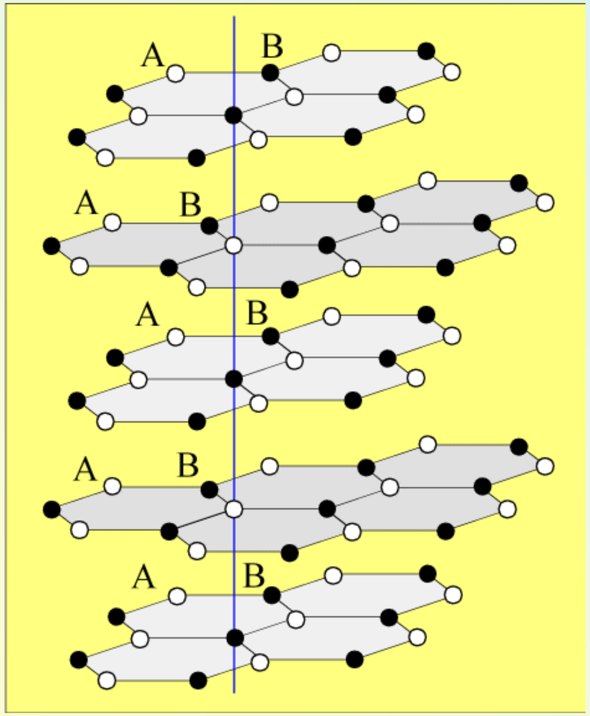

Layered poorly conducting semimetal used in pencils and nuclear fusion moderators

M. Dresselhaus, G. Dresselhaus
Adv. Phys. 51, 1 (2002)

Buckyballs

Curl, Kroto
Smalley 1985

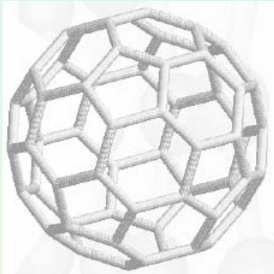

Nanotubes

Iijima 1991
Smalley 1993

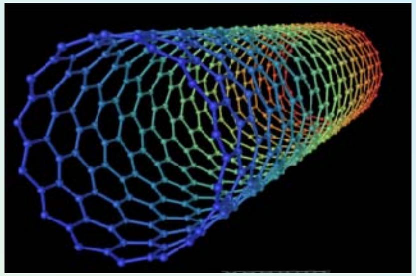

'Theoretical graphene'

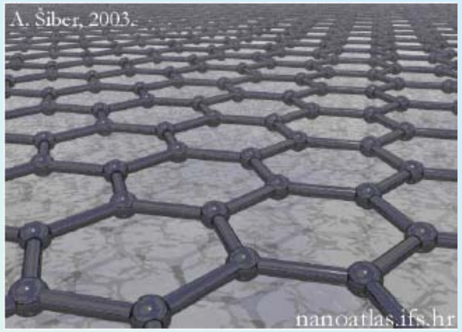

construction block in the theory of graphite and nanotubes

Physical Properties of Carbon Nanotubes
Saitoh, Dresselhaus, Dresselhaus, Imperial College Press 1998